A NUMERICAL MODEL FOR IMPACTS OF LEFT-TURN NON-MOTORIZED VEHICLES ON THROUGH LANE CAPACITY METRICS

Lieyun HE[1], Xinming LIN[2], Qiang LIU[3], Jason X. TAO[4]

[1] *Department of Transportation Management and Engineering, Zhejiang Police Collage, China*

[2] *International School, Zhejiang Police Collage, China*

[3] *Big data-based Key Laboratory of the Ministry of Public Security, Zhejiang Police College, China*

[4] *Washington D.C. Department of Transportation, USA*

Abstract:

There is a conflict between through motor vehicles and the left-turn non-motorized vehicles, and the capacity of straight-line motor vehicles decreases. This study analyzes the impacts of left-turn non-motorized vehicles on the capacity of through motor vehicle lanes. A correction coefficient model for calculating the reduced capacity of through motor vehicle lanes has been developed based on analysis of the conflicting points at an intersection and the negative exponential function of traffic flow distribution. With consideration of intersection geometric design, channelization, and traffic characteristics, the correction coefficient model was further enhanced by regression to capture the impacts of left-turn non-motorized vehicles from the same and the opposite directions. A simulation with VISSIM is used to validate the developed model. It shows that the calculated capacity from the correction coefficient model is close to the simulation results. The experiment indicates that the derived model is highly accurate in calculating the capacity of through motor vehicle lanes and has potential application for situations of mixed traffic in China. The study shows that the capacity of a through traffic lane at the permitted phase decreases with the increase of left-turning non-motorized vehicles, and the impact of left-turning non-motorized vehicles from the same direction is more significant. The results show that the traffic capacity of straight-line motor vehicle decreases with the increase of the left-turn non-motorized vehicles flow rate and the influence of the left-turn non-motor vehicle is more obvious. It is suggested that in practice, the correction coefficient of non-motor vehicle on the left turn should be 0.88, and the correction coefficient on the left turn should be 0.95, respectively. The study recommends coefficient values for both non-motorized vehicles from the same and opposite directions for use in real applications.

Keywords: traffic design, signalized intersection, permissive phase, traffic lane capacity, regression analysis

To cite this article:

Contact:

1) helieyun@zjjcxy.cn [https://orcid.org/0000-0002-8316-2333] – corresponding author, 4) jtao2013@gmail.com [https://orcid.org/0000-0002-8871-5144] – corresponding author

1.   Introduction

The way traffic is managed and controlled at signalized intersections directly affects the capacity and safety of intersections. There are two basic approaches to manage left-turn non-motorized vehicle traffic at signalized intersections. One is to mix low speed non-motorized vehicles with motor vehicles in the same directions. The other is to mix traffic of low speed non-motorized vehicles with pedestrians. Mixing traffic of non-motorized vehicles with pedestrians is not common in practice due to the fact that non-motorized vehicles can pose severe danger to pedestrians. Mixing low-speed non-motorized vehicles with motor vehicles at intersections is more common as it fits the habits of transportation participants (Yang et al., 2012). Based on different methods of controlling left-turn traffic, signal control can have three types: a protective phase control, a permissive phase control, and a protective + permissive phase control. Each type can be applied to two-phase intersections, four-phase intersections, and intersections with overlapped phases. At signalized intersections with permissive left-turn phases, there exist many conflicts between motor vehicles and non-motorized vehicles. In these situations, the conflict between through motor vehicles and left-turn non-motorized vehicles is particularly significant. All of these conflicts affect the capacity and safety of intersections (Shi et al., 2013). Further research on the impacts of left turn non-motorized vehicles on the capacity of motor vehicle traffic at intersections is important for enhancing signal design and improving traffic management and operations.

In Highway Capacity Manual (HCM2010), the basic saturated flow rate is set as 1900pub/h/lane, while 7 basic saturation flow adjustment coefficients are given to calculate highway capacity. It also provides the adjustment coefficients for the left and right turn flows to capture the impacts of pedestrians and bicycles, and the time ratio of a protective phase. Yang et al. (2018) analyzed the characteristics of conflicts between right-turn vehicles, pedestrians, and non-motorized vehicles. He proposed the pedestrian adjustment coefficients as an enhancement to the Highway Capacity Manual approach. Based on the characteristics of bicycle traffic flow at intersections, Sun and Yang (2004) developed traffic capacity models for both types of mixed traffic – mixed traffic of motor vehicle and non-motorized vehicles,

and mixed traffic of non-motorized vehicles and pedestrians. In order to reduce traffic delays caused by conflicts between different types of vehicles from different directions at intersections, some researchers proposed a traffic management model for continuous flows at intersections (Jagannathan and Bared, 2005; Tanwanichkul et al., 2015; Tarko et al., 2010). Along this direction, Zhao et al. (2018) proposed an optimal design for left-turn non-motorized vehicles to minimize their impacts on the through traffic as an enhancement to the conventional continuous intersection design. On the evaluation of the main operation of intersections, scholars at home and abroad mainly adopt the delay time, queue length, parking times and so on (Zhao et al., 2018). Chen et al. (2008) established a simulation model with the VISSIM software to study the impact of non-motorized vehicles on capacity of intersections.

By reviewing past research, the following drawbacks have been identified in the previous studies: (1) Human powered bicycles are considered as main non-motorized vehicles in developing traffic capacity models. However, in recent years the proportion of electric bicycles in non-motor vehicle traffic has been increasing. Electric bicycles are very different from human-powered bicycles in vehicle parameters, running speed, acceleration, deceleration and other characteristics; (2) It is often assumed that motor vehicles and left-turning non-motor vehicles arrive randomly at the intersection, and left-turn non-motorized vehicles pass the conflict points through the gap of through motor vehicle traffic from the same direction. This assumption may not be valid as the drivers of through motor vehicles may yield to non-motorized vehicles and pass the conflict points through the gap of left-turn non-motorized vehicle flows; (3) It is often assumed that non-motorized vehicles arrive as continuous traffic flows in analyzing the conflicts between motor vehicles and non-motorized vehicles. These studies are focused on analysis of the right-turn capacity. However, in reality, non-motor vehicles are more likely to present the characteristics of interrupted flows and that the through motor vehicle lane should be the key lane in capacity analysis. The capacity of the through motor vehicle lane should be paid more attention in intersection design. In this paper, we apply the probability theory of traffic flow and regression analysis to establish a capacity adjustment coefficient model to

capture the impacts of left-turn non-motorized vehicles during permissive phases. VISSIM simulation software is used to analyze the accuracy of the proposed model.

2. Traffic flow characteristics at signalized intersections with a permissive left-turn phase during green light

As shown in Figure 1, a typical orthogonal signalized intersection is considered in this study. We assume that both north-bound and south-bound directions have permissive left-turn phases for motor vehicles and non-motorized vehicles. Traffic from the south is the focus of this analysis. During phase green time, the north-bound through motor vehicles have two conflict points, A_1 and A_2, as shown in Figure 1. A_1 is the conflicting point caused by left-turn vehicles from the same direction, and A_2 is the conflicting point caused by left-turn vehicles from the opposite direction. Based on the traffic flow characteristics for the intersection with permissive left-turn phase, the green time of the permissive phase can be divided into four stages $T_1 \sim T_4$. The definitions of these stages are described below.
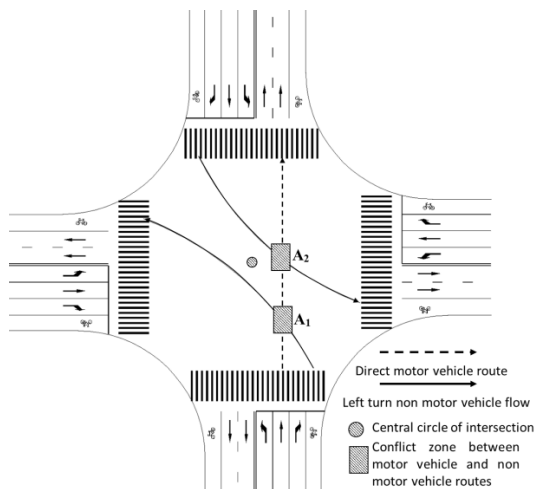
Fig. 1. An intersection with conflicting traffics of through motor vehicles and left-turn non-motorized vehicles during a permissive left-turn phase

2.1. T_1: a stage that left-turn non-motorized vehicles from the south pass through the conflicting zone A_1 as saturation flow

Due to its flexibility in driving and lighter weight, a non-motorized vehicle has greater acceleration in starting when compared to a regular motor vehicle. A non-motorized vehicle experiences shorter stopped delay. In addition, some non-motorized vehicles tend to stop beyond the stop line during the phase red time. In stage T_1, non-motorized vehicles arrive earlier at the conflict zone A_1 than motor vehicles. After passing through the stop line, through motor vehicles will stop again in front of the conflicting zone A_1, and then move to pass the zone after all non-motorized vehicles pass through the conflict zone A_1. At this stage, motor vehicles passing through the stop line will experience stopped delay twice.

2.2. T_2: a stage that through motor vehicles pass through the conflict zone A_1 and A_2 as saturation flow

By the end of stage T_1, the queue of left-turn non-motorized vehicles from the southern direction dissipates, and the through motor vehicles pass through the conflict zone A_1 and A_2 in a platoon. At this stage, left-turn non-motorized vehicles from the opposite direction will queue up before the conflicting zone A_2 and wait to pass after the platoon of through motor vehicles disappear and the through motor vehicles arrive randomly.

2.2. Stage T_3 - stage that left-turn non-motorized vehicles from the opposite direction pass through the conflicting zone A_2 as saturation flow

After stage T_2, through motor vehicles and non-motorized vehicles from the southern direction will enter the intersection randomly, and the left-turn non-motorized vehicles from the opposite direction will wait before passing through the conflict zone A_2 in a platoon. If time duration that left-turn non-motorized vehicles from opposite direction use to pass through the conflicting zone A_2 is longer than the headway of the through motor traffic flow, then the through motor vehicles will stop and queue up in front of the conflicting zone A_2 again. The observation shows that the probability for a through motor vehicle to stop again before the conflicting zone A_2 is very small.

2.3. T_4: A stage during which through motor vehicles and left-turn non-motorized vehicle in the southern direction pass through the conflicting zones randomly

If the total time of the first three stages (T_1, T_2 and T_3) is less than the green time of the north-south phase, the phase indication will still be green, and all non-motorized vehicles will arrive at the intersection randomly after the platoons of through motor vehicles and left-turn non-motorized vehicles from the southern and the opposite direction disappear. At stage T_4, through motor vehicles move across the conflicting zones A_1 and A_2 through the gaps of left-turn non-motorized vehicles from the southern and the opposite direction.

3. A model to calculate the capacity for through vehicle flows at intersections with permissive phases

There are three major existing approaches to calculate the capacity of intersections: The first approach is based on the saturation flow rates and correction coefficients. This approach found in the Highway Capacity Manual (TRB, 2000; Zhang et al., 2013) from the United States and in China's regulations for roadway (GB, 2011) represent the research in this direction. The second approach is the stop line based method (Zhang and He, 2014), in which vehicles that pass through the stop line are considered to have left the intersection. The third approach is the conflicting point based approached proposed by Xu et al. (2001), in which only those vehicles that have passed through the conflicting areas are considered to have left the intersection. These three approaches apply to different traffic flow conditions. The saturation flow -based approach does not apply to intersections with mixed traffic flows of motor vehicles and non-motorized vehicles. The stop line -based approach is more applicable to intersections with mixed traffic flows of motor vehicles and non-motorized vehicles where protected phases are implemented. This paper studies the conflicts between motor vehicles and non-motorized during the green time of left-turn permissive phases and its impacts on the intersection capacity.

It is assumed in the model that the arrivals of motor vehicles and non-motorized vehicles follow the Poisson distribution. Assuming that the vehicle arrival rate from the north bound entrance of the intersection as in Figure 1 is λ (pub/h), the arrival rate of left-turn non-motorized vehicles from the north bound entrance of the intersection is $λ_{sb}$ *(bic/h)*, and the arrival rate of left-turn non-motor vehicles upstream of the south bound entrance is $λ_{nb}$ *(bic/h)*, the cycle length of this intersection is C, and the green time of the north-south phase is G_{snr}. The model is described in the following sections:

3.1. The capacity for the through motor vehicles during stage T_1

During stage T_1, the number of non-motorized vehicles passing through the conflicting zone A_1 follows:

$$Q_{BST1} = Q_{NS} \times T_1 \times (\eta \times w_S - 0.5) \tag{1}$$

Where Q_{BST1} is the number of non-motorized vehicle (unit: pub) passing through the conflicting zone A_1 during stage T_1. Q_{NS} is the flow rate of non-motorized vehicle $bic/(s \cdot m)^{-1}$, the value of that is within the range of $0.28 \sim 0.33 bic \cdot (s \cdot m)^{-1}$ [13]. η is the inflation coefficient for left-turn non-motorized vehicles. Its value is set to 2.1 in mixed traffic conditions with both motor vehicles and non-motorized vehicles (Yuan and Yuan, 2006). w_S is the lane width of the north-bound non-motorized vehicle lane (m).

The number of non-motorized vehicles, Q_{BST1}, that pass through the conflicting zone A_1 during stage T_1 can also be calculated as:

$$Q_{BST1} = λ_{sb} \times (C - Gsnr) \tag{2}$$

Based on equations (1) and (2), the duration of the first stage, T_1, can be obtained as follows:

$$T_1 = \frac{λ_{sb} \times (C - Gsnr)}{Q_{NS} \times (\eta \times w_S - 0.5)} \tag{3}$$

In stage T_1, since the non-motorized vehicle move at saturation flow rate, the number of motor vehicles C_{T1} that pass through the conflicting zone A_1 can be ignored, that is, $C_{T1} = 0$.

3.2. The capacity for through motor vehicles during stage T_2

During stage T_2, through motor vehicles are not affected by left-turn non-motorized vehicles. Through motor vehicles pass through the conflicting zone in a platoon during this stage. The number of vehicles

C_{T2} that pass the stop line during T_2 is the number of through vehicles that arrive at the intersection either during the phase red light or during the stage T_1:

$$C_{T2} = \lambda \times (C - Gsnr + T_1) \qquad (4)$$

The duration of stage T_3 can be calculated as:

$$T_2 = \frac{C_{T2}}{\tau_c} \qquad (5)$$

where τ_c is the average headway of through vehicles passing through the stop line as saturation flow. Its value is related to the type of motor vehicles at the intersection. When traffic is composed of only small motor vehicles, $\tau_c \approx 2.5S$. The value of τ_c in a mixed traffic varies according to the proportion of vehicles type (Zhang and He, 2014).

3.3. The capacity of through motor vehicles during stage T_3

Similarly, according to equation (3), the duration of the stage T_3 can be obtained as:

$$T_3 = \frac{\lambda_{nb} \times (C - Gsnr)}{Q_{NS} \times (\eta \times w_N - 0.5)} \qquad (6)$$

where w_N is the lane width of the south-bound non-motorized entry lane (m). If the time gap between two successive through motor vehicles, h, is greater than or equal to T_3, the movement of the through motor vehicles will not be blocked by left-turn non-motorized vehicles. According to the law of negative exponential distribution, the probability of a through motor vehicle that can pass through the conflicting zone is:

$$P(h \geq T_3) = e^{-\lambda_{nb} T_3} \qquad (7)$$

The total number of through motor vehicles that pass through the conflict zone is:

$$C_{T3} = \lambda \times T_3 \times e^{-\lambda_{nb} T_3} \qquad (8)$$

3.4. The capacity for through motor vehicles in stage T_4

As shown in Figure 2, we use h_{sb} to denote the headway of left-turn non-motorized vehicles from the southern direction, h_{nb} to denote the headway of left-turn non-motor vehicles from the opposite direction. α is also used to denote the minimum headway for a through motor vehicle to cross the left-turn non-motor traffic from the southern and opposite directions. α_o denotes the minimum headway for through motor vehicles successively to pass through the conflicting zone. The number of through motor vehicles that pass through the conflicting zone in stage T_4 is:

$$C_{T4} = \sum_{k=1}^{n} \lambda_{sb} T_4 P_k \times k \\ + \lambda T_4 \lambda_{sb} e^{-n\lambda_{sb}(\alpha + n\alpha_o)n} \qquad (9)$$

where k is the number of through motor vehicles that pass through the conflicting zone (pub), P_k is the probability that k vehicles from the queue are able to pass through the conflicting zone, N is the maximum number of motor vehicles that the through lanes can accommodate (pub).

Equation (9) can be simplified to:

$$C_{T4} = T_4 \times \frac{\lambda_{sb} e^{-\lambda_{sb}\alpha}(1 - e^{-\lambda_{sb} n\alpha_o})}{1 - e^{-\lambda_{sb}\alpha}} \qquad (10)$$

When $n \to \infty$, the overflow of traffic on guiding through lanes will not occur, thus the number of vehicles that pass through the conflicting zone during stage T_4:

$$C_{T4} = T_4 \times \frac{\lambda_{sb} e^{-\lambda_{sb}\alpha}}{1 - e^{-\lambda_{sb}\alpha}} \qquad (11)$$

The duration of stage T_4 is:

$$T_4 = Gsnr - \sum_{i=1}^{3} T_i \qquad (12)$$

In summary, the algebraic expression of the number of vehicles that pass through the intersection during the green light period is:

$$C_T = \sum_{i=1}^{4} C_{T_i} = \lambda[(C - Gsnr + T_1) \\ + T_3 e^{-\lambda_{nb} T_3}] + T_4 \frac{\lambda_{sb} e^{-\lambda_{sb}\alpha}}{1 - e^{-\lambda_{sb}\alpha}} \qquad (13)$$

where C_T is the number of through motor vehicles that pass through the intersection in a signal cycle, in pub/C, and the capacity of the through lanes is:

$$C_T = \frac{g_i}{C} \cdot S_o \cdot \prod f \cdot f_{slb} \cdot f_{slb} \qquad (14)$$

where g_i is the effective green time (s) of the phase for the through traffic; S_o is the basic capacity of the through lane (pub/h); $\frac{g_i}{C} \cdot S_o$ is the saturation flow rate of the through lane; $\prod f$ is the saturation flow rate correction coefficient of through lane without considering the influence of left-turn non-motorized vehicle traffic; f_{slb}、 f_{nlb} are the correction coefficients for left-turn non-motorized vehicle from the southern and opposite directions, respectively. According to equation (14), the left-turn correction coefficient model can be established as:

$$f_{slb} \cdot f_{slb} = \frac{C \times C_T}{g_i \times S_o \times \prod f} \qquad (15)$$

From formula (15), it can be seen that the factors influecing the correction coefficient of left-turn non-motor vehicles include the upstream arrival rate of non-motorized vehicles from the southern and opposite directions, the flow rate of non-motorized vehicles, the lane width of non-motorized vehicle entrance lane, and the inflation coefficient for non-motorized vehicles at the intersection.

4. A regression analysis on the correction coefficient model for left-turn non-motorized vehicles

The intersection shown in Figure 2 is still used in the regression analysis. Based on the intersection design and traffic flow characteristics at intersections with left-turn permissive phases, the related parameters are set as follows: the lane width of the left-turn non-motorized lane is 2.5m; the inflation coefficient for non-motorized traffic at intersections is 2.1; the basic capacity of the through lane at the north-bound entrance is 1650 pub/h, that is, the saturated flow rate is 655pub/h. The flow rate of non-motor vehicle is $0.305\text{bic}/(s \cdot m)^{-1}$; The minimum headway of left-turn motorized vehicles that allows a through-vehicle to pass through is 5s. The phase times can be found in Table 1 in this analysis.
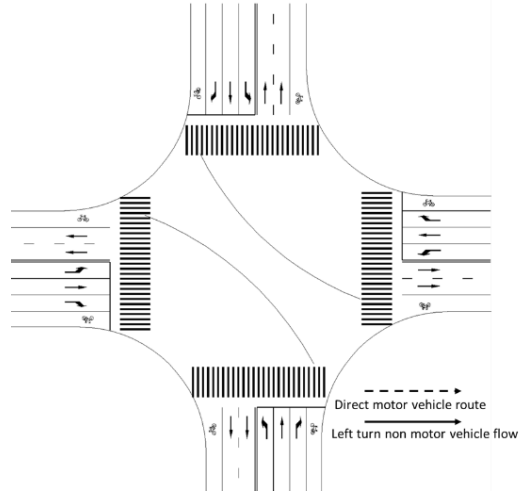
Fig. 2. A diagram of through motor vehicle crossing the intersection between the gaps of left-turn non-motorized vehicles during permissive phase green time

4.1. A correction coefficient model for left-turn non-motorized vehicle

Based on the above traffic flow parameters, let $\prod f = 1$, that is, only the impacts of the left-turn non-motorized vehicles on through traffic is considered. The correction coefficient f_{slb}、 f_{nlb} are expressed as:

$$f_{slb} \cdot f_{nlb} = \frac{C \times C_T}{g_i \times S_o \times \prod f} \qquad (16)$$

When the arrival rate of left-turn non-motorized vehicles $\lambda_{nb} = 0$, left-turn non-motorized vehicles will not affect the through traffic, that is, $f_{nlb} = 1$. Under such condition, the correction coefficient model for non-motorized vehicles from the southern direction is:

$$f_{slb} = \frac{C \times C_T}{g_i \times S_o} \qquad (17)$$

4.2. A fitting curve for the left-turn non-motorized vehicle correction coefficient

We calculated the corresponding f_{slb} by inputting the different values of λ_{sb} into equation (17). In this experiment, the range of λ_{sb} is $50\text{bic/h} \leq \lambda_{sb} \leq$

1000bic/h with a step length of 50bic/h. A regression analysis on the values of f_{slb} was conducted by using the Matlab software. The results are shown in Figure 3. Various functions including an exponential function, a linear function, a logarithmic function, a quadratic function, and a power function were tried in fitting curve. It was found that a quadratic function fit the results best as the R-square value is almost equal to 1. f_{slb} can be expressed as a regression quadratic function:

$$f_{slb} = 1.2\lambda_{sb}^2 - 1.1\lambda_{sb} + 1 \qquad (18)$$

The scattered point diagram of the correction coefficient f_{nlb} for non-motorized vehicles from the opposite direction is obtained using a similar approach, as shown in Figure 4. The R-square value in a regression with a quadratic function f is 0.9993. f_{nlb} can be expressed as a quadratic function:

$$f_{nlb} = -1.2\lambda_{sb}^2 + 1 \qquad (19)$$

The unit of non-motorized vehicle arrival rate is *bic/s* in equations (17) and (18). According to the results of this experiment, the average value of the correction coefficient for left-turn non-motorized vehicles from the southern direction is 0.88, meaning that the impact of left-turn non-motorized vehicles from this direction on through traffic is significant.

Other the other hand, the average value of the correction coefficient for left-turn non-motorized vehicles from the opposite direction is 0.97. This means that the impact of left-turn non-motorized vehicles from the opposite direction on north-bound traffic is relatively small.

5. An analysis on the model accuracy with VISSIM simulation

5.1. Parameter settings for the simulation analysis

The VISSIM simulation software was used to evaluate the accuracy of the left-turn non-motorized vehicle correction coefficient model (Wojtal and Rilett, 2017). To ensure that simulation results are comparable to the regression analysis, all parameters such as intersection type, vehicle type, signal phasing, timing parameters, and the features of the conflicting zone in the simulation are set to the same values as in the regression model. Figure 5 illustrates an example of an intersection where the width of through lanes is 3.5m and the width for the non-motorized vehicle lane is 2.5m. The condition of $\prod f = 1$ is satisfied with these settings. A vehicle counting station is put on the exiting through lanes after the conflicting zone A_2 to collect the volume of through traffic that pass through the conflicting zones.

Table 1. Intersection signal timing plan

Signal Plan	Cycle Length	Green time for the east-west direction phase	Green time for the east-west phase	Yellow time
Two phase	70s	32s	32s	3s
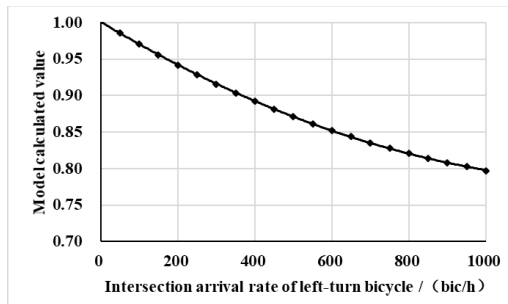
Fig. 3. Calculated values for the correction coefficient for the left-turn motorized vehicles
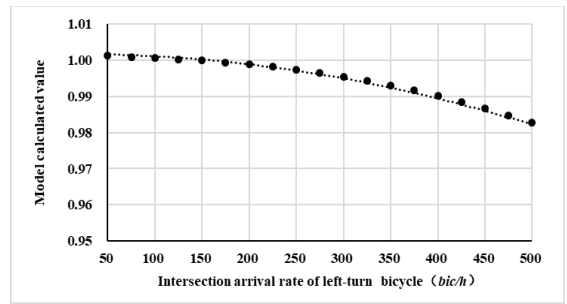
Fig. 4. Calculated values for the correction coefficient for the left-turn motorized vehicles from the opposite direction
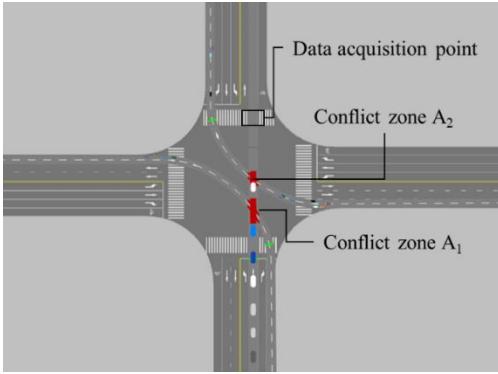
Fig. 5. The Intersection Settings for the Simulation

A saturation flow rate of 682pub/h on through lanes was obtained after changing the input flow rate several times. This value is used as the input flow rate of through motor vehicles. The mean speed of motor vehicles is set as *60km/h*, and the mean speed of the non-motorized vehicles is set as *20km/h*. The value range of non-motorized vehicle flow rates and the step size used in the simulation analysis are consistent with that in the regression analysis. Through the simulation, the value of the correction coefficient for left-turn non-motorized vehicles from the same direction, f_{sslb}, can be obtained based on equation (17). A scatter diagram of f_{sslb} is drawn with the Matlab software, as shown in Figure 6.

Similarly, we can obtain the values of the correction coefficient for left-turn non-motorized vehicle from the opposite direction, f_{snlb}, from the simulation. A scatter diagram of f_{snlb} is shown in Figure 7. By comparison, the values of coefficients calculated through the regression model are relatively steady,

while the values from the simulation have stochastic variations due to different settings of vehicle type.

5.2. Accuracy analysis of the capacity correction coefficient

The accuracy of the correction coefficient model can be evaluated through error assessment, which includes assessment of individual errors and the overall error. The individual error indices include absolute error (AE) and relative error (APE), while the overall error indices include mean relative error (MAPE) and root mean square error (RMSE) (Zhu et al., 2018). In this paper, AE, MAPE, and RMSE are selected to analyze the accuracy of the model. The calculation formulas for these indices are as follows:

$$AE = \frac{1}{n}\sum_{i=1}^{n}|X_i - X_i'| \qquad (20)$$

$$MAPE = \frac{1}{n}\sum_{i=1}^{n}\left|\frac{X_i - X_i'}{X_i}\right| \times 100\% \qquad (21)$$

$$RMSE = \sqrt{\frac{1}{n}\sum_{i=1}^{n}(X_i - X_i')^2} \qquad (22)$$

where X_i is the simulation values of the correction coefficient for left-turn non-motorized vehicles, X_i' is the calculated value of the correction coefficient for left-turn non-motorized vehicle from the analytical model, n is the sample size. The results of the error indices are shown in Table 2.
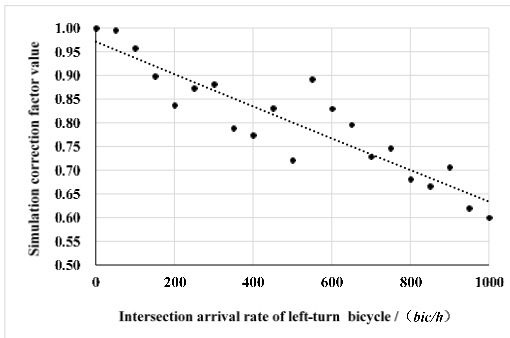
Fig. 6. A scatter diagram of correction coefficient for left-turn bicycles from the same direction
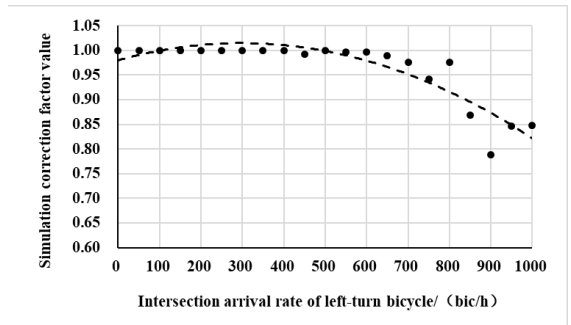
Fig. 7. A scatter diagram of correction coefficient for left-turn bicycles from the opposite direction

Table 2 An Error Analysis on the Correction Coefficient Model

Direction of non-motorized vehicle entrance	AE	MAPE	RMSE
From the same direction	0.038	4.8%	0.10
From the opposite direction	0.026	3.0%	0.05

The small error values in Table 2 indicate that the correction coefficient model for left-turn non-motorized vehicle developed in this study achieved high accuracy in calculating the capacity impacted by left-turn non-motorized vehicles. The model provides a theoretical basis for traffic design and traffic operations at intersections with permissive left-turn phase.

6. Conclusion

The conflicts between left-turn non-motorized vehicles and through motor vehicles at intersections can significantly reduce the capacity of the through motor vehicles at intersections with permissive phases. A numerical equation for calculating capacity was derived based on the analysis of conflicting points and traffic flow characteristics. The correction coefficient model for left-turn non-motorized vehicles was established by regression analysis, and the accuracy of the model was verified by the VISSIM simulation. The results of error analysis showed that the model achieved high accuracy in calculating the capacity. The developed model can provide insights for intersection design improvements, traffic control, and traffic management.

The results show that the capacity for through motor vehicles under a permissive phase is significantly affected by left-turn non-motorized vehicles from the same direction. The impact of left-turn non-motorized vehicles from the opposite direction is small and can be ignored. In practice, we suggest the correction coefficient for left-turn non-motorized vehicles from the same direction be 0.88, and the correction coefficient for left-turn non-motorized vehicles from the opposite direction be 0.95. These values can be applied to signalized intersections where data for left-turn non-motorized vehicles is not available.

References

[1] YANG, X., YANG, J., SHI, Y., 2012. *Non-motorized Vehicle Left-turn Design at Signalized Intersections*. Urban Transport of China, 10(04), 65-71+18.

[2] SHI, Y., YANG, X., YANG, J., 2013. *Comparative Research on Traffic Design Patterns of Urban Road Intersection*. Traffic & Transportation, 01, 54-57.

[3] YANG, X., ZHU, X., BAI, Y., 2018. *Modeling the Impacts of Pedestrian and Non-mobile on the Left-turn Capacity of Signalized Intersections with Permitted Left-turn Phasing*. China Transportation Review, 40(07), 53-58.

[4] SUN, M., YANG, X., 2004. *Research on the Theory of Traffic Design for Intersection of Mixed Traffic*. Journal of Highway and Transportation Research and Development, 08, 82-86.

[5] JAGANNATHAN,, R., BARED, J., 2005. *Design and performance analysis of pedestrian crossing facilities for continuous flow intersections*. Transportation Research Record, 1939, 133-144.

[6] TANWANICHKUL, L., PITAKSRINGKARN, J., BOONCHAWEE, S., 2015. *Determining the optimum distance of continuous flow intersection using traffic microsimulation*. Journal of the Eastern Asia Society for Transportation Studies, 9, 1670-1683.

[7] TARKO, A., AZAM, S., INEROWCIZ, M., 2010. *Operational performance of alternative types of intersections a systematic comparison for Indiana conditions*. Congress Proceedings, 32(31), 386-391.

[8] ZHAO, J., XU, H., GAO, X., WANG, T., 2018. *Optimization Design Method of Left-turn Bicycles Crossing for Continuous Flow Intersections*. Journal of Transportation Systems Engineering and Information Technology, 18(06), 178-186.

[9] ZHAO, H., HE, R., SU, J., 2018. *Multi-objective optimization of traffic signal timing using*

non-dominated sorting artificial bee colony algorithm for unsaturated intersections. Archives of Transport, 46(2), 85–96.

[10] CHEN, X. SHAO, C. YAO, Z., 2008. *A Study on successive crossings of left-turn bicycles at typical signalized intersections.* China Civil Engineering Journal, 07, 76-81.

[11] TRB, 2000. TRANSPORTATION RESEARCH BOARD., 2000. *Highway Capacity Manual, Special Report 209.* Washington D C: National Research Council.

[12] ZHANG, S., REN, G., YANG R., 2013. *Simulation Model of Speed -Density Characteristics for Mixed Bicycle Flow-Comparison between Cellular Automata Model and Gas Dynamics Model.* Physica A, 392 (10), 5110-5118.

[13] GB, 2011. *GB 50647－2011 Code for planning of intersections on urban roads., 2011.* Beijing. China Planning Press.

[14] ZHANG, S., HE, K., 2014. *Expansion Effect of Left Turning Mixed Bicycle Flow and Vehicle-Bicycle Conflict at Intersections.* Journal of Ningbo University of Technology, 26(02), 7-11.

[15] XU, L.,WU, C., YANG, Z., 2001. *The Methods of Computing the Capacity of Signalized Intersection.* Journal of Traffic and Transportation Engineering, 01, 82-85.

[16] YUAN, J., YUAN, Z., 2006. *Comparison Analysis of Calculation Methods for Traffic Capacity at Signal Junction.* Technology of Highway and Transport, 05, 123-128+132.

[17] WOJTAL, R. M., RILETT, L. R., 2017. *Development of a statistically-based methodology for analyzing automatic safety treatments at isolated high-speed signalized intersections.* Archives of Transport, 44(4), 75-88.

[18] ZHU, X. GUO, J. HUANG, W. YU, F. PARK, B., 2018. *Real-time Short-term Forecasting Method of Remaining Parking Space in Urban Parking Guidance Systems.* Promet Traffic & Transportation, 30(2), 173-185.